Available online at www.sciencedirect.com
SCIENCE DIRECT®
Thermochimica Acta 403 (2003) 1–13
thermochimica acta
www.elsevier.com/locate/tca

The thermal properties of complex, nanophase-separated macromolecules as revealed by temperature-modulated calorimetry☆

Bernhard Wunderlich [a,b,*]

[a] *Department of Chemistry, University of Tennessee, Knoxville, TN 37996-1600, USA*
[b] *Oak Ridge National Laboratory, Chemical Sciences Division, Oak Ridge, TN 37831-6197, USA*

Received 5 September 2002; received in revised form 16 January 2003; accepted 17 January 2003

Abstract

Linear, flexible macromolecules are long recognized as phase structures limited to micrometer and nanometer dimensions with covalent bonds crossing the interfaces. This special, usually non-equilibrium structure leads to unique properties and a multitude of changes for different thermal and mechanical histories. Analyses that enable the study of these properties are temperature-modulated calorimetry and related techniques which allow the separation of equilibrium and non-equilibrium responses. Research on these topics is reviewed and combined to a model for the nanophases. The new approach to the complex nanophase systems yields a better understanding of the relationship between structure and thermodynamic properties. Special emphasis is placed on the size and surface effects on the glass and melting transitions, the development of rigid-amorphous phases, and the reversible melting within the globally metastable structure.
Published by Elsevier Science B.V.

Keywords: Nanophase; DSC; TMDSC; Flexible polymers; Non-equilibrium thermal properties; Thermal history; Mechanical history; Reversible melting; Rigid-amorphous fraction; Molecular nucleation

1. Introduction

Temperature-modulated differential scanning calorimetry (TMDSC) originated in the early 1990s [1–3] and has become by now an established technique of thermal analysis. Its development can be followed by the discussions held during the last four biannual Lähnwitz Seminars in 1994–2000. At the Third Lähnwitz Seminar, in 1994, we reported on "Modulated DSC—Capabilities and Limits." This lecture dealt with early developments to describe the experimental basis and data treatment for the conditions of steady state in the calorimeters and negligible temperature gradients within the sample [4,5]. The broad spectrum of presentations from the Fourth Lähnwitz Seminar to the present are published in collected volumes of *Thermochimica Acta* and represent an important resource of the state of development of TMDSC [6]. Our contributions consisted of the "Heat Capacity Determination by Temperature-Modulated DSC and its Separation from Transition Effects" [7],

☆ Presented at the Seventh Lähnwitz Seminar. This manuscript has been authored by a contractor of the US Government under the contract no. DOE-AC05-00OR22725. Accordingly, the US Government retains a non-exclusive, royalty-free license to publish or reproduce the published form of this contribution, or allow others to do so, for US Government purposes.

* Present address: 200 Baltusrol Road, Knoxville, TN 37922-3707, USA. Tel.: +1-865-675-4532; fax: +1-865-675-4532.
E-mail address: wunderlich@chartertn.net (B. Wunderlich).

0040-6031/03/$ – see front matter. Published by Elsevier Science B.V.
doi:10.1016/S0040-6031(03)00099-6

the "Temperature-Modulated Differential Scanning Calorimetry of Reversible and Irreversible First-Order Transitions" [8], and "Measurement of Heat Capacity to Gain Information About Time Scales of Molecular Motion from Pico to Megaseconds" [9]. In the Fourth Lähnwitz Seminar, the discussion centered about the methods of heat-capacity measurement and the special problems that arise from the glass transition. Even without an enthalpy of transition, deviations from linearity were observed and could be linked to the kinetic parameters of the process [10–13]. Also, at the Fourth Lähnwitz Seminar [7] a new observation was reported. Quasi-isothermal TMDSC shows a reversing contribution to polymer melting [14–17]. This was surprising since flexible, linear macromolecules should melt irreversibly [18]. More detailed research could be presented at the Fifth Lähnwitz Seminar [8]. It involved the study of the first-order transitions of small and large molecules [19,20]. Our next research topic concerned with TMDSC was the simultaneous modulation with several frequencies. It showed how the loss of steady state in sawtooth modulation could be handled [8]. The development of this topic led then to the invention of complex sawtooth modulation [21] which can be generated even with a standard DSC, and was tested in heat-flux calorimeters with modulations that were controlled at the position at the sample [22] or at the heater [23] and in power-compensation calorimeters [24]. The results permitted not only the analysis of time-dependent processes in a single experiment, but also eliminated the need for negligible temperature gradients within the sample by means of an internal calibration. The presentation for the Sixth Lähnwitz Seminar was used to elucidate the time scales of importance to classical and time-dependent calorimetry [9]. The molecular motions are the ultimate time-dependent processes in materials, and it is easy to represent the atomic motion by molecular dynamics simulations using supercomputers [25]. It was even possible to connect calorimetry directly to molecular motion, which ultimately may lead to "Thermal Analysis via Molecular Dynamics Simulation" [26]. It was shown that it is important to handle time scales from picoseconds to megaseconds (10^{-12} to 10^{6} s), where a megasecond covers a measuring time of about 2 weeks.

Another 2 years have past, and at the Seventh Lähnwitz Seminar we were excited about the fact that TMDSC of reversible melting and rigid-amorphous phases of over 25 semicrystalline macromolecules [27] has led to the conclusion that most of their observed behavior can be traced to the nanophase structure [28]. In this paper we will try to resolve the oxymoron of nanophases which must be homogeneous, but on approach to atomic dimensions will become heterogeneous.

2. Nanophases and macromolecules

The main topic in this section is the understanding of "phases" and their changes with decreasing size. Traditionally, the term phase is defined thermodynamically as a state of matter that is uniform throughout, not only in chemical composition, but also in physical state. In other words, a phase consists of a homogeneous, macroscopic volume of matter, separated by well-defined surfaces of negligible influence on the phase properties [29]. Domains in a sample that differs in chemical composition or in physical state are considered to be different phases.

Atoms and molecules, first recognized on an experimental basis by Dalton [30], are the basic elements of the phases, i.e. it is commonly assumed that phases which reach atomic dimensions cannot be described by thermodynamics because of insufficient statistical elements to define the functions of state. In the last century enough information about the structure of molecules was collected to permit the separation of all matter into three types of molecules, as summarized in Fig. 1 [31]. This separation was made to underline the connection of molecular size to the possible phases. While small molecules may be found in all three classical phases, large molecules may not. The distinction between small and large molecules was made by Staudinger [32,33] who also coined the term "macromolecule." Rigid macromolecules keep their integrity only in the solid state. On fusion or melting, the molecular structure is destroyed and the macromolecules break into smaller entities. Flexible, large molecules, in turn, may be sufficiently mobile by rotation about nonlinear bonds to permit transitions from the solid to the liquid without loss of molecular integrity.

The key transition to be discussed involves the change between solid and liquid and is based on the

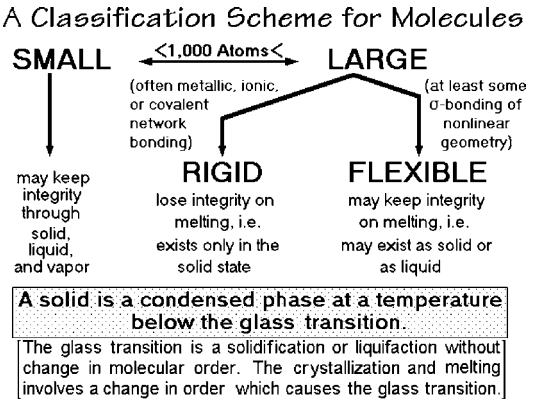

Fig. 1. Summary of the classification of molecules based on their phase properties and a description of the solid–liquid transitions.

loss of large-amplitude motion, such as are found in translational, rotational, and conformational changes of location. Of particular interest is the relationship between the glass transition and the melting transition. On vitrification, the cooperative, large-amplitude motion of the molecules freezes without change in the phase structure. On crystallization, the molecules order, but the ordering causes also the freezing of the cooperative, large-amplitude motion as in the glass transition. Melting is usually seen at a higher temperature (T_m) than the glass transition temperature (T_g). Mesophases with intermediate degrees of order also have a T_g, unless they crystallize when cooled [34].

Similar to the change in molecular size, the change in size of the phases causes distinct differences. Summarized in Fig. 2, the macrophase can be described

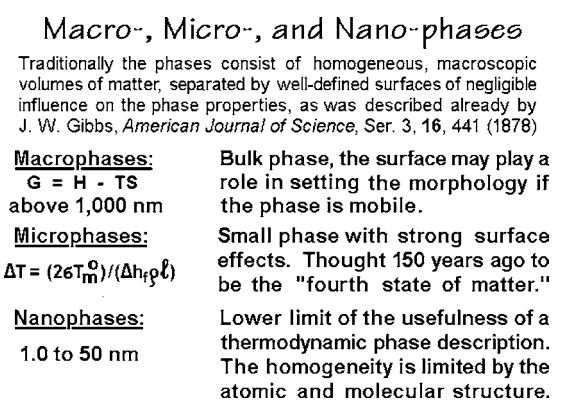

Fig. 2. Classification of phases according to size.

by the integral thermodynamic functions enthalpy (H), entropy (S), and free enthalpy (G). The influence of the surface free energy (σ) is negligible. Its function is only of importance in the liquid state where it minimizes the surface area, and during the crystallization where it fixes the crystal morphology [18].

Microphases, which have phase dimensions of less than 1 μm, where discovered in form of colloids some 150 years ago [35] and were called erroneously "a fourth state of matter" [36]. This label is better reserved for the plasma, represented in physics by an electrically conducting fluid phase with close-to-equal numbers of positive ions and electrons with properties quite distinct from the solid, liquid, and gaseous states. Colloids do not represent new states of matter, but are well-known phases, just of much smaller size. For the description of microphases, the surface free energy is pivotal. Colloids, for example, are usually kept from growth to larger particles by a surface charge. Crystalline microphases, as common in lamellar crystals of flexible linear macromolecules, have a distinctly lower melting temperature, as given by the Gibbs–Thomson equation which is listed in Fig. 2. The specific surface area of the lamellae is $2\sigma/\ell$, where ℓ is the lamellar thickness. For this equation to be valid, it is assumed that the lateral surface is negligible. The term $\Delta h_f \rho$ represents the enthalpy of fusion per unit volume with ρ representing the density. Similar to T_m, one expects T_g to be affected by the size of the phase.

Nanophases are suggested in Fig. 2 to have dimensions between 50 and 1 nm. They reach the lower limit of applicability of thermodynamics caused by the atomic structure of matter. The upper limit is variable, and is approached whenever bulk material with properties of the macrophase appears in the center of the nanophase. In other words, in a nanophase, the surface effects change the properties throughout the phase.

Having established the phase size, it is necessary to match phase and molecular size. For small molecules and large phases, the phase volume can easily accommodate all molecules. Flexible macromolecules, however, are typically 1000–100,000 chain atoms long, which corresponds for the example of polyethylene to a molar mass of 14,000–1,400,000 Da, respectively, or a contour length within the crystal of 127 nm to 12.7 μm. For microphases and nanophases of flexible

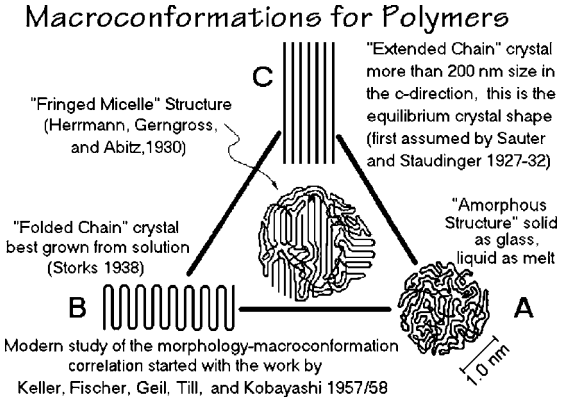

Fig. 3. Summary of macroconformations of flexible polymers.

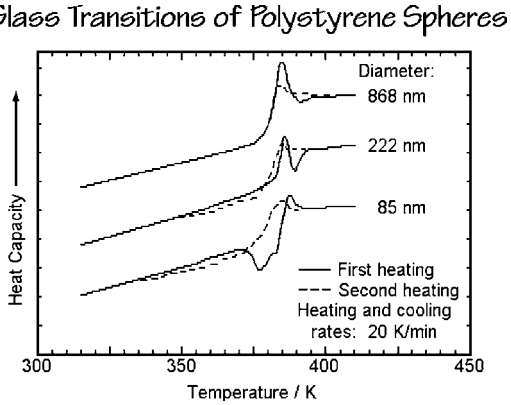

Fig. 4. Change of the glass transition of polystyrene with decreasing size of the phase.

macromolecules, thus, the molecules may cross the interfaces and cause a strong coupling between neighboring phases.

To fit macromolecules into a phase of given morphology, the shape of the molecule must be known. Fig. 3 is a summary of the basic shapes of flexible, large molecules, their so-called macroconformations [18]. The radius marker of 1.0 nm for the amorphous droplet would correspond to a single polyethylene molecule of only about 10,000 molar mass, i.e. it represents the border between small and large molecules as given in Fig. 1. The folded-chain crystals have typically a lamellar thickness of 10–50 nm, i.e. long, perfectly crystallized molecule may have as many as 1000 folds. The extended-chain crystals would need a crystal thickness of the contour length of the molecules. In most cases, macromolecules order to a semicrystalline structure, as is sketched in the center of the triangle as a fringed micellar macroconformation. It is a typical nanophase structure with strong coupling between the phases and contains elements of all three limiting macroconformations. In the following sections the thermal properties of such nanophase-separated macromolecules are discussed, as revealed by DSC and TMDSC.

3. Size and surface dependence of glass transitions

An early discussion of the size dependence of amorphous microphase and nanophase structures was given on the example of polystyrene and poly(styrene-*block*-α-methystyrene) [37]. Fig. 4 illustrates the changes in the glass transition of small spheres of polystyrene as they approach nanophase dimensions when measured by standard DSC. The diameters were measured by electron microscopy. On first heating, the beginning of the glass transition of smaller spheres occurs at lower temperature, while the midpoint of the heat-capacity increase shows little changes. The exotherm visible on first heating is typical for the stress released on coalescing of the spheres. For the smallest spheres this occurs below at the beginning of the glass transition. To analyze the change in the transition with size, the samples coalesced above the glass transition were heated again after cooling, to provide a baseline for the bulk polymer.

Fig. 5 illustrates the calculation of the volume of the respective spheres that were affected by the reduction in size. The change in ΔC_p suggests that a 5 nm layer has a gradually decreasing glass transition. For the spheres of 868 nm diameter, such a small amount of material is outside the error limit. For the spheres of 85 nm, one can match the experimental change in glass transition when assuming that the glass transition changes by about 8.0 K/nm as one approaches the outer surface for the last 5 nm, as illustrated in Fig. 6. Based on these experiments and the above attempt of definitions, a nanophase of amorphous polystyrene spheres would be reached at a diameter of about 10 nm, the diameter of disappearance of bulk material in their center. Similar conclusions

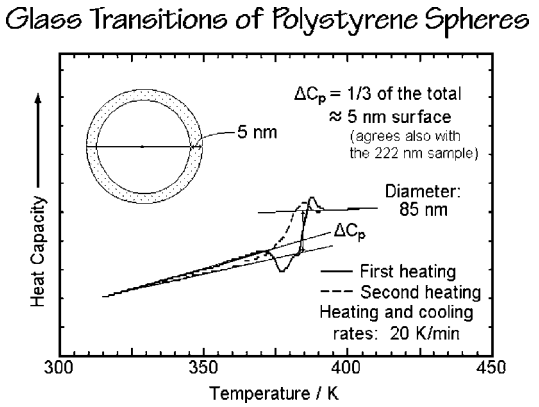

Fig. 5. Analysis of the data of Fig. 4.

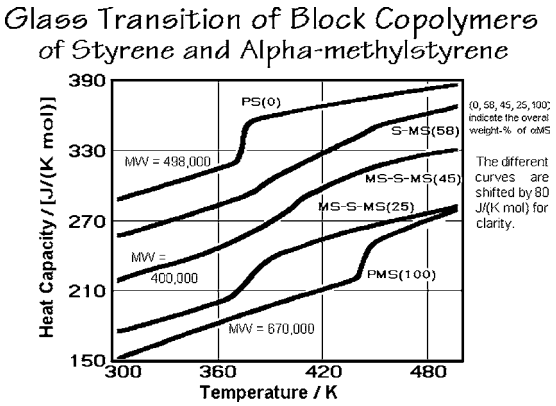

Fig. 7. Glass transitions of phase-separated block copolymers.

were reached more recently, based on model calculations and Brillouin light scattering data on thin free standing films of polystyrene down to 20 nm [38].

In the lamellar, phase-separated structures of block copolymers, a similar broadening of the glass transitions is visible in Fig. 7 [37]. The glass transition of the styrene blocks is broadened towards higher temperature, and that of the α-methylstyrene, towards lower temperature. Under proper conditions, the measurement appears like a single glass transitions. Electron microscopy, however, proves the two-phase, lamellar nature of all samples, and DSC can document hysteresis peaks centered at each of the two homopolymer glass transitions. The increase of the T_g of the styrene blocks is caused by the glassy environment created by the α-methylstyrene blocks which are still below their glass transition, while the decrease of the glass transition of the α-methylstyrene blocks is enabled by the lower glass transition of the surrounding styrene blocks. Assuming that both effects are similar in absolute magnitude to the effect of the free surface on the polystyrene spheres in Fig. 4, one can produce the plot of the change of the beginning or end of the glass transitions, given in Fig. 8. The temperature T_b is the beginning of the glass transition of the α-methylstyrene blocks and the polystyrene spheres, and T_e, the end of the glass transition of the styrene blocks. The effect is continuous with specific surface area, i.e. the phase size determines the glass transition temperature [37].

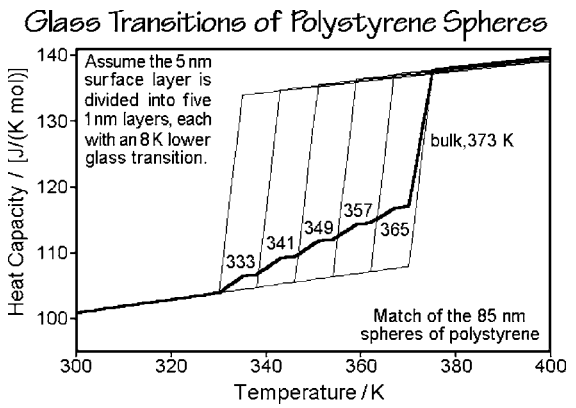

Fig. 6. Synthesis of the experimental data of Fig. 4.

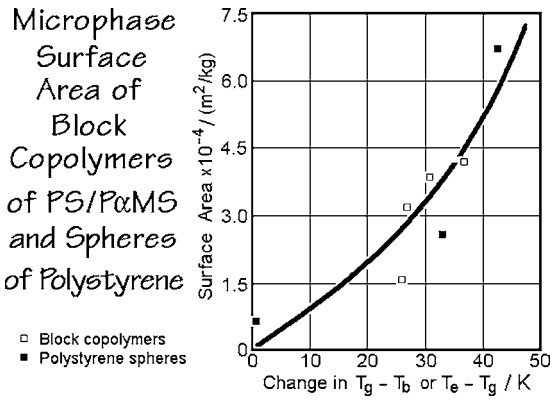

Fig. 8. Increase and decrease of the glass transition as a function of specific surface areas, derived from data of Figs. 4 and 7.

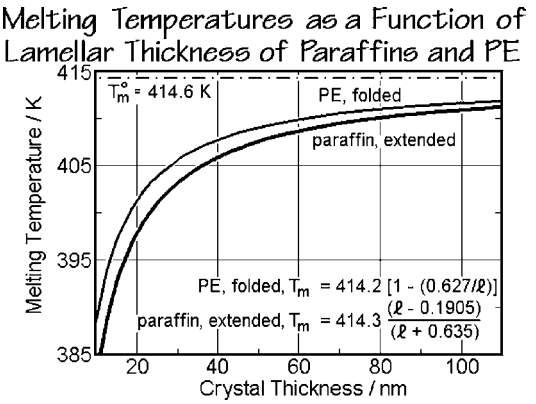

Fig. 9. Melting temperatures of lamellar crystals.

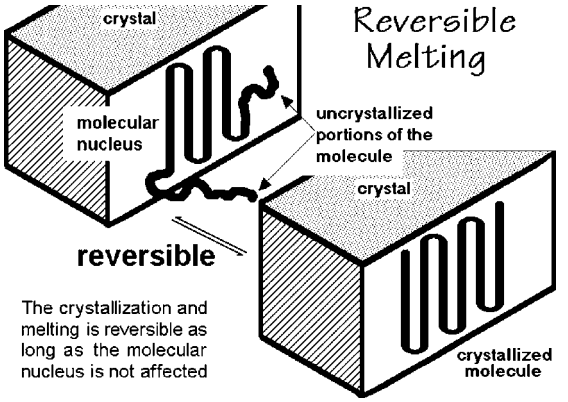

Fig. 10. Schematic of reversible melting based on the melting temperatures of Fig. 9.

4. Size and surface dependence of melting transitions

The effect of the size of the phase in crystalline polymers is also known for a long time. Since the thickness of the lamellar crystals, ℓ, reaches also into the microphase and nanophase range, one can plot the lowering of the melting temperature, ΔT, as a function of $1/\ell$, as required by the Gibbs–Thomson equation, listed in Fig. 2. Fig. 9 illustrates the result based on a large number of folded-chain crystals of known ℓ, analyzed by DSC under zero-entropy-production conditions, i.e. avoiding crystal perfection during the analysis ([18], vol. 3, p. 32). Also listed in the Fig. 9 are the experimental melting temperatures of paraffins as a function of their molecular contour length ([18], vol. 3, p. 26). Both curves meet at the equilibrium melting temperature of polyethylene, 414.6 ± 0.5 K, also determined experimentally [39].

Fig. 10 demonstrates that the separation of the size-dependent melting temperature of extended-chain paraffins and folded-chain polyethylene is of importance for the interpretation of local nanophase equilibria in an overall system of metastable crystals. Treating portions of a molecular chain on the surface of a crystal as a decoupled nanophase, their melting temperatures are less than those of the central part of the folded-chain molecule. Once the whole molecule is melted, recrystallization of polyethylene needs commonly a supercooling of about 7–9 K to overcome the free enthalpy barrier for molecular nucleation. During an analysis with TMDSC, the decoupled chain portions can then melt reversibly, several kelvins below the irreversible melting temperature of the rest of the molecule because the remaining center of the molecule serves as a molecular nucleus. A similar scenario can be developed for a chain end which is decoupled through a loose loop, originating in the interior of the crystal, or a tie molecule connecting to another crystal of higher, irreversible melting temperature. The model can also be extended to decoupled chain ends that contain several chain folds, with melting temperatures approaching the high-molar-mass limit in Fig. 9 as the number of folds increases [40].

The remaining question about the melting of flexible molecules is the limit of small molecule crystallization which is usually only hindered by crystal nucleation. Fig. 11 reveals the need of molecular nucleation for paraffins, and polyethylenes of increasing chain lengths beyond a molecular contour length of about 10 nm ($x \approx 75$) [41,42]. A sample with low molar mass components can melt reversibly, although there may also be a time dependence due to the need to separate the various fractions into eutectic crystals. Pure paraffins, such as $C_{50}H_{102}$, melt for this reason reversibly, while the fraction PE560 shows some degree of irreversibility, i.e. the total apparent heat capacity is not fully identical to the reversing apparent heat capacity because of the time needed for separation of the melt into different crystals for each species [42]. The breadth of the eutectic melting range increases with decreasing average molar mass, as can be derived from T_m of the paraffins in Fig. 9.

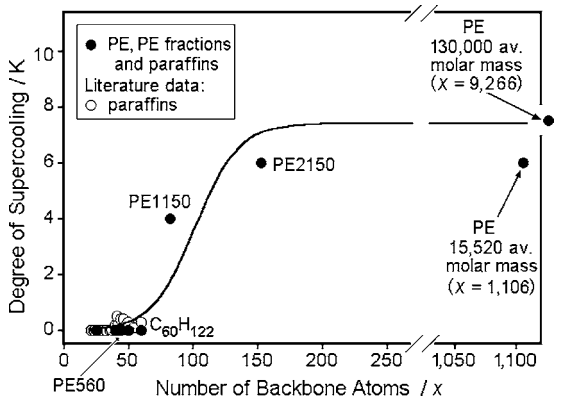

Fig. 11. Change of the supercooling on crystallization with molecular length for paraffins, polyethylene fractions (designated by their molar masses as PE560, PE1150, and PE2150), and polyethylene homopolymers, PE (of the indicated average molar masses). The average numbers of carbon atoms are given by *x*.

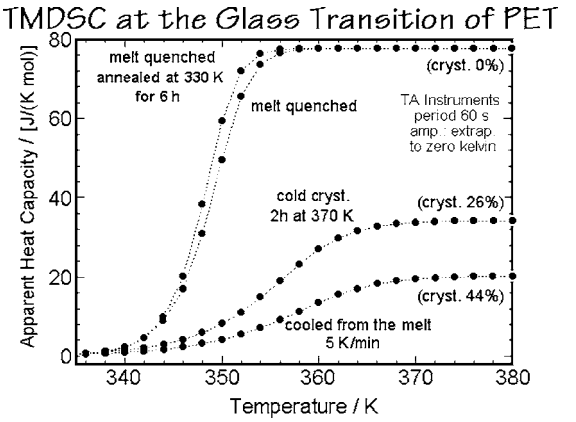

Fig. 12. Quasi-isothermal TMDSC of poly(ethylene terephthalate) of different crystallinity.

5. Glass transition in non-equilibrium phase structures

Semicrystalline polymers contain crystalline microphases and nanophases, as well as noncrystalline material in an overall metastable structure. Metastability is best proven by the violation of the phase rule which allows for only one phase a one-component system in equilibrium and at constant pressure outside of the melting temperature and forbids semicrystallinity. Assuming fringed micellar macroconformation, as in the center sketch of Fig. 3, one expects a size effect not only in the melting temperature of the crystals, as seen in Fig. 9, but also in the glass transition, as in Fig. 8. In Fig. 12, quasi-isothermal data by TMDSC are shown for poly(ethylene terephthalate)s of different crystallinity [12]. The glass transition of the semicrystalline samples is broadened to higher temperature relative to the amorphous samples, similar to the styrene segments of the block copolymer in Fig. 7. An interface to the crystal acts as the restriction for motion in the glass.

In addition, an inspection of the increase of the heat capacity during the glass transition (ΔC_p), in Fig. 12 seems not to agree with the crystallinity which is deduced from the heat of fusion. Since the heat capacity is linked quantitatively to the vibrational spectrum and the conformational motion, it is a material property and should be conserved. A deficit in the ΔC_p, thus, points to an additional phase, called the "rigid-amorphous fraction" (RAF) [43]. Fig. 13 is a summary of a thermal analysis of poly(oxymethylene). The deficit between the calculated ΔC_p of the 67% crystalline sample and the measured ΔC_p, which points to an 80% solid content, results in 13% RAF. Since the RAF shows no relationship to the glass transition of the bulk-amorphous phase, one can assume that it is a nanophase with its own glass transition. Examples are known where the glass transition of the RAF occurs between the glass transition of the bulk-amorphous phase and T_m, but most often it occurs together with the melting transition. The second graph in Fig. 13 illustrated the effect of the RAF on the heat

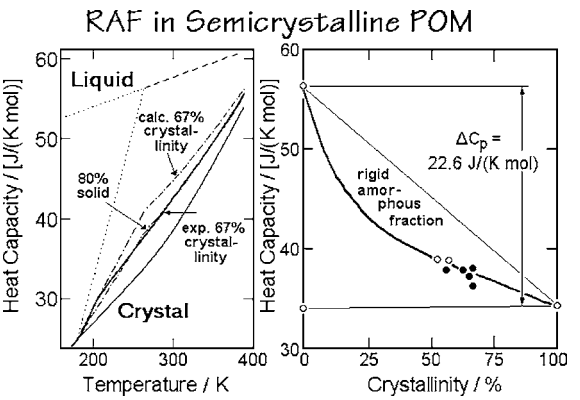

Fig. 13. Heat-capacity change in the glass transition region, illustrating the presence of a rigid-amorphous fraction (RAF).

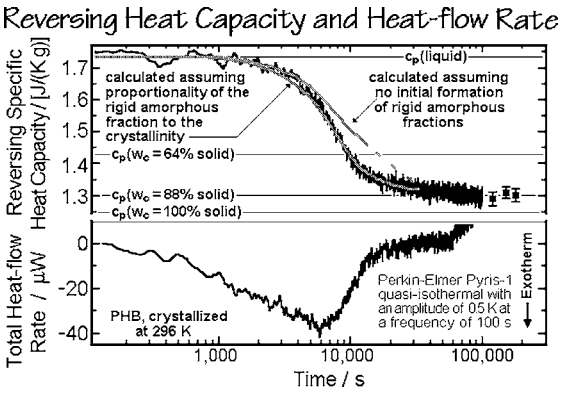

Fig. 14. Formation of the rigid-amorphous fraction on crystallization for poly(hydroxy butyric acid) [45].

capacity over the full crystallinity range. Changes in crystal morphology as produced by a different history of crystallization, produce additional variations in the amount of RAF. A detailed model of such three-phase has been worked out by Mathot and Ruiten [44].

The TMDSC experiments of Fig. 14 are proof that in the case of poly(3-hydroxybutyrate) (PHB) the RAF is produced alongside the crystals. If it were a product of the later impingement of the crystals, the calculated change in heat capacity with crystallinity could not match the measured change in reversing, apparent specific heat capacity [45].

A rare case of an RAF with a glass transition above the melting temperature is illustrated with DSC experiments on poly(oxy-2,6-dimethyl-1,4-phenylene) (PPO) [46], with Fig. 15. A case analyzed recently

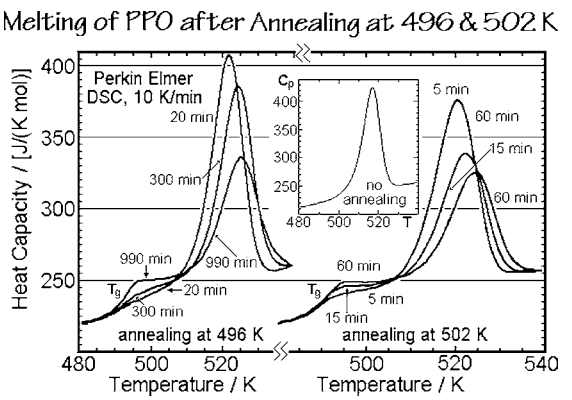

Fig. 15. Reduction of the rigid-amorphous fraction on melting for poly(oxy-2,6-dimethyl-1,4-phenylene).

with TMDSC [47]. The standard DSC trace of a semicrystalline sample in the center plot of the figure shows no glass transition of the bulk-amorphous phase, i.e. all noncrystalline PPO is RAF. It is, however, possible to anneal the sample below the melting range and to produce a bulk-amorphous glass transition with a simultaneous decrease in melting peak area, as shown by the other traces in Fig. 15. Since the second law forbids the melting of crystals below their zero-entropy-production melting temperatures, this must mean that the glass transition of the RAF is in this case above the melting temperature, but melting is retarded since the crystals are enclosed in the glassy RAF. Melting is only possible after the RAF becomes mobile. A quantitative analysis of melting and glass transition by TMDSC has shown that the major part of melting goes parallel to the devitrification of the RAF [47]. Not only is the RAF created parallel with the crystals, as shown in Fig. 14, it also disappears parallel with the melting, as shown in Fig. 15. Any discussion of melting and crystallization, thus, must also include the fate of the RAF.

6. Reversible melting in non-equilibrium phase structures

In this final section on nanophases of polymers, the melting of polyethylene will be summarized as an example of a most complex behavior. Much more information in the often simpler reversible melting of other polymers of different degrees of flexibility has recently been summarized [27]. The first surprising observation was a reversible lamellar thickness of the polyethylene crystals when changing the temperature [48,49]. This result defies the application of the Gibbs–Thomson equation of Fig. 2, according to which the thinner crystals should be less stable and once thickened, should not become thin again. Next, it was shown that semicrystalline polyethylene has an intermediate nanophase of lesser mobility than the amorphous phase covering the fold surfaces of the crystals. The proof required element-specific transmission electron microscopy on RuO_4-stained samples [50]. This third phase was preferentially stained and appeared on both sides of the crystalline lamellae and was linked to the reversible change of the lamellar thickness. These direct observations were also connected to the

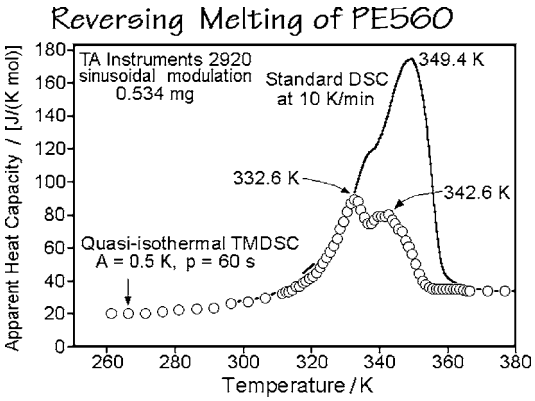

Fig. 16. Total and reversible melting of a low-molar-mass fraction of polyethylene.

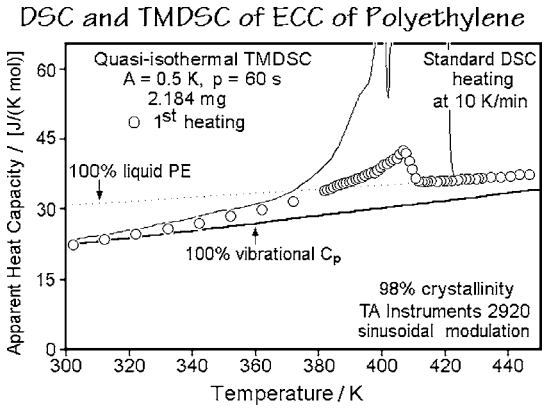

Fig. 17. Total and reversible melting of an extended-chain sample of 98% crystalline polyethylene.

20–30% of the sample with an intermediate mobility between the amorphous and crystalline PE seen from spin-lattice relaxation of ^{13}C solid state NMR. The glass transition of the intermediate phase, however, is not separated from the bulk glass transition of polyethylene, but only shows a broadening of the transition range to higher temperature. Recently, TMDSC and time-resolved, temperature-modulated wide- and small-angle X-ray diffraction could identify similar reversible changes in crystal thickness [51].

A connection to the fully reversibly melting paraffins could be made for the low-molar-mass fraction of polyethylene, PE560 of Fig. 11. No supercooling was found since the molar mass is below the critical length for nucleation. Fig. 16 reveals, however, that the total apparent heat capacity as measured by DSC and the reversing heat capacity as determined by quasi-isothermal TMDSC do not agree over the whole melting range, even when taking into account the considerable lag in standard DSC [42]. The specific reversibility, defined as the ratio of the reversible melting per kelvin to the total melting per kelvin, both at the same temperature, changes from 1.0, as expected for full reversibility, to less than 0.5 [52]. The main reason for the partial irreversibility is not molecular nucleation, since the molecules are below the critical length of Fig. 11, but the large amount of readjustment of the concentration in the melt by slow diffusion needed for the adjustment for the crystal distribution with temperature dictated by the eutectic phase diagram [42]. The first reversible melting peak at 332.6 K may be an indication of the eutectic temperature range.

An increase of the average molar mass to PE1150, PE2150, and the polymer PE130000 in the extended-chain crystal morphology the specific reversibility decreases drastically as shown in Fig. 17. The sample was crystallized at elevated pressure, to reach the extended-chain morphology and its crystallinity was 98%. The total reversibility, when integrated over the whole melting range, is only 7%, of which almost half belongs to the fraction in the sample with a molar mass below the critical value of Fig. 11 with a melting temperature below 385 K. This is followed by a rapidly decreasing fraction of reversibility of the crystals melting up to 408 K, belonging to the 22% of the sample of higher molar mass which are still segregated according to chain length. The final fraction of 73% of the crystals melts with very little reversibility up to 409.5 K, and none up to the melting end of 411 K [53]. Indeed, narrow fractions of extended-chain crystals of polyethylene, as well as several aliphatic polyoxides, are among the polymers of very little reversible melting [27].

Polyethylenes of folded-chain morphology, as seen in sample PE15520, for example, have a much higher reversibility than the extended-chain crystals. The most reversible melting can be seen in linear, low-density polyethylenes of the type used for the analysis of Fig. 18 [19]. Recent quantitative TMDSC analyses found a specific reversibility of 0.8–0.6 from room temperature down to the glass transition [52]. In the polymer of Fig. 18, this covers all the crystals grown outside the sharp primary crystallization peak

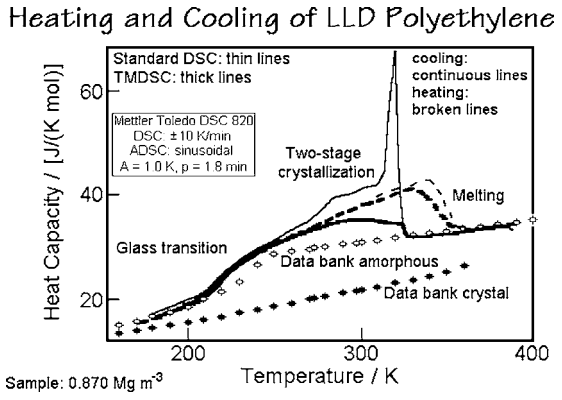

Fig. 18. Total and reversing melting and crystallization of a particular linear low-density polyethylene.

which also have a more pseudo-hexagonal crystal structure of smaller heat of fusion [19,20,54]. On heating, the specific reversibility remains of the order of magnitude of 0.5 well into the melting peak for the copolymers as well as for homopolymers, a sign that the mechanisms of reversible and irreversible melting are related, as suggested by Fig. 10. Recent ^{13}C NMR analyses of similar ethylene-1-octene copolymers with ethylene could show a separation of the polyethylene crystals formed by longer ethylene sequences from two noncrystalline phases. One, the amorphous phase, containing side chains and short methylene sequences, the other a less mobile phase which is enriched by methylene and methine groups of the main chain [55]. The reversibly melting nanophases at low temperature should be at the interfaces between the crystals and the less mobile amorphous phase. Two mechanisms seem possible, the one based on the folded-chain surfaces, discussed at the beginning of this section, and the other occurring as the only mechanism in polymers that show no fold-surface mobility on the growth faces [27]. A similar complication of the melting of polyethylene crystals was observed for gel-spun, linear polyethylene, where three phases of different order, mobility, heat of fusion, and orientation could be identified and linked to the mechanical properties [56,57].

7. Discussion and conclusions

While during the last few Lähnwitz Seminars data gained with temperature-modulated calorimetry and related techniques were at the center of the discussions, the present seminar highlighted a standard technique able to heat with rates of hundreds of kelvins per minute, new techniques measuring with integrated-circuit devices, Peltier heating and cooling, heating with modulated illumination, and resistance heating with AFM tips, often capable to measure nanojoule quantities of heat on small sample volumes and at frequencies of measurement up to possibly 100 Hz [58]. The results from such techniques concentrating on very small samples need to be supported by definitive descriptions of the limits of macrophases (>1.0 μm), microphases (between 1.0 μm and 50 nm), and nanophases (between 50 and 1.0 nm) (Fig. 2) and the connection of these phases to the molecular sizes (Fig. 1) and macroconformations (Fig. 3). The structure–property relationships can be linked to the effects caused by changes in size and interaction on solidification, seen in the glass and melting transitions. Both transitions are based on cooperative freezing and unfreezing of conformational motion, the first without change in order, the second, with.

Decreasing phase dimensions with either free surfaces or mobile interfaces moves the beginning of the glass transition to lower temperature, as illustrated by Figs. 4–8. Related changes were also reported on thin films and samples enclosed in small pores [58]. Strong interactions across an interface increases the end of the glass transition, as seen in microphase-separated copolymers with one component of higher T_g as shown in Figs. 7 and 8. Crystalline lamellae of folded and extended macroconformations similarly decrease in T_m with decreasing thickness.

The model of reversible crystallization displayed in Fig. 10 relies on the assumption that portions of the macromolecules may be decoupled, i.e. they can be treated as a separate phase. This important topic was documented with a discussion of side-chain macromolecules with side chains of sufficient length to form their own nanophase with a separate glass transition [58]. Similar observations documented side-chain melting temperatures similar to their equivalent short-chain molecules [18]. This decoupling of chain segments has been largely neglected in the past description of the phase behavior of polymers. It may not only be of importance for the understanding of the local equilibria in an overall metastable polymer system, but also hold the key in the discussion of

the melting and glass transitions of copolymers. A decoupled chain segment, for example, which cannot increase its entropy of melting due to diffusion into areas of higher concentration of the noncrystallizable component, will approach T_m of the homopolymer of similar phase size. The question of simultaneous or coupled physical and chemical processes in thermodynamics should gain importance in the future and must be included in models for polymeric thermodynamic systems as discussed during the seminar [58]. Another experimental observation in need for a detailed theoretical model is the critical chain length for reversible melting displayed in Fig. 11. One expects this critical chain length to be time-dependent and quantitative TMDSC may shed more light on the crystallization process. Such analysis would be of importance since some of the recently proposed intermediate stages of crystallization in the form of spinodally decomposed phases of different degrees of chain extension and possible transient mesophase formation may not agree with the here documented locally reversible thermal properties [59].

The behavior of the noncrystalline phase in semicrystalline polymers, as illustrated in Figs. 12–15 links not only the broadening of the glass transition to the block copolymers imbedded in a glassy second phase, as given in Figs. 7 and 8, but with Figs. 12 and 13 it also documents the existence of a third phase, the RAF. The RAF may have its T_g within the broadened bulk transition, have a separate T_g below T_m, or at T_m, and even a T_g above T_m, is possible. The RAF is a nanophase with properties different from the bulk-amorphous due to the strong interaction across its interface.

The TMDSC and DSC experiments of Figs. 14 and 15 prove that in the analyzed cases the RAF is produced along with the crystals, and also disappears along with the crystals. These experiments are taken as proof that the interface causing the different noncrystalline properties is that to the crystal. Further details of the formation of the RAF, its size and the kinetics of its glass transition are accessible through TMDSC and are of importance for the understanding of the influence of the RAF on the properties of semicrystalline polymers.

The last group of Figs. 16–18 represents the reversible melting of polyethylene. Similar effects are seen in other flexible macromolecules [27]. The increase in heat capacity due to conformational motion is seen in all paraffins and polyethylenes and has also been found in several aliphatic polyoxidses. In case of possible sliding diffusion in the crystal, it may induce a small reversibility of lamellar thickness [27]. Fig. 16 documents limiting reversibility due to slow attainment of the phase equilibrium, despite of a molar mass less than the critical value for reversibility. Increasing the molar mass of extended-chain crystals makes the melting irreversible. Only a small amount of reversibility remains for somewhat broader molar-mass distributions and whenever the crystallinity does not approach 100%, as was discussed on hand of Fig. 17. This remaining degree of reversibility is likely due to diffusion effects and crystal defects coupled with local amorphous phases [18,25]. The copolymer of Fig. 18 with low polyethylene crystallinity, finally, illustrates in its primary crystallization and melting the reversibility, typical of folded-chain crystals, linked to the model of Fig. 10. Down to the glass transition reversible, local melting is caused by small crystals which are limited in size by the copolymer units.

In conclusion, the existence of a metastable, global structure in flexible polymers with local equilibria involving nanophases and microphases, often based on decoupled chain segments, is at the center of the structure–property relationship. The development of new calorimetric techniques able to help in the study of these small-phase structures, their reversibility and kinetics are producing experiment-based progress in the understanding of this unique class of materials. Much further information for the different types of polymers are expected in the future, as concluded from the extended discussions of this Lähnwitz Seminar [58].

Acknowledgements

This work was supported by the Division of Materials Research, National Science Foundation, Polymers Program, Grant #DMR-9703692 and the Division of Materials Sciences and Engineering, Office of Basic Energy Sciences, US Department of Energy at Oak Ridge National Laboratory, managed and operated by UT-Battelle, LLC, for the US Department of Energy, under contract number DOE-AC05-00OR22725.

References

[1] M. Reading, Trends Polym. Sci. 8 (1993) 248.
[2] M. Reading, D. Elliot, V.L. Hill, J. Therm. Anal. 40 (1993) 949.
[3] P.H. Gill, S.R. Sauerbrunn, M. Reading, J. Therm. Anal. 40 (1993) 931.
[4] B. Wunderlich, Y. Jin, A. Boller, Thermochim. Acta 238 (1994) 277.
[5] A. Boller, Y. Jin, B. Wunderlich, J. Therm. Anal. 42 (1994) 307.
[6] Thermochim. Acta 304–305 (1997); 330 (1999); 377 (2001).
[7] B. Wunderlich, A. Boller, I. Okazaki, K. Ishikiriyama, Thermochim. Acta 304–305 (1997) 125.
[8] B. Wunderlich, A. Boller, I. Okazaki, K. Ishikiriyama, W. Chen, M. Pyda, J. Pak, I. Moon, R. Androsch, Thermochim. Acta 330 (1999) 21.
[9] B. Wunderlich, M. Pyda, J. Pak, R. Androsch, Thermochim. Acta 377 (2001) 9.
[10] A. Boller, C. Schick, B. Wunderlich, Thermochim. Acta 266 (1995) 97.
[11] B. Wunderlich, A. Boller, I. Okazaki, S. Kreitmeier, J. Therm. Anal. 47 (1996) 1013.
[12] I. Okazaki, B. Wunderlich, J. Polym. Sci., Part B: Polym. Phys. 34 (1996) 2941.
[13] L.C. Thomas, A. Boller, I. Okazaki, B. Wunderlich, Thermochim. Acta 291 (1997) 85.
[14] I. Okazaki, B. Wunderlich, Macromolecules 30 (1997) 1758.
[15] I. Okazaki, B. Wunderlich, Macromol. Chem. Phys., Rapid Commun. 18 (1997) 313.
[16] K. Ishikiriyama, B. Wunderlich, Macromolecules 30 (1997) 4126.
[17] K. Ishikiriyama, B. Wunderlich, J. Polym. Sci., Part B: Polym. Phys. 35 (1997) 1877.
[18] B. Wunderlich, Macromolecular Physics, Crystal Structure, Morphology, Defects Crystal Nucleation, Growth, Annealing Crystal Melting, vols. 1–3, Academic Press, New York, 1973–1980.
[19] R. Androsch, B. Wunderlich, Macromolecules 32 (1999) 7238.
[20] R. Androsch, B. Wunderlich, Macromolecules 33 (2000) 9076.
[21] B. Wunderlich, R. Androsch, M. Pyda, Y.K. Kwon, Thermochim. Acta 348 (2000) 181.
[22] M. Pyda, Y.K. Kwon, B. Wunderlich, Thermochim. Acta 367–368 (2001) 217.
[23] J. Pak, B. Wunderlich, Thermochim. Acta 367–368 (2001) 229.
[24] Y.K. Kwon, R. Androsch, M. Pyda, B. Wunderlich, Thermochim. Acta 367–368 (2001) 203.
[25] B.G. Sumpter, D.W. Noid, G.L. Liang, B. Wunderlich, Atomistic dynamics of macromolecular crystals, Adv. Polym. Sci. 116 (1994) 27.
[26] S.N. Kreitmeier, G.L. Liang, D.W. Noid, B.G. Sumpter, Thermochim. Acta 46 (1996) 871.
[27] B. Wunderlich, Progress Polym. Sci. 28 (2003) 383.
[28] W. Chen, B. Wunderlich, Nanophase separation of small and large molecules, Macromol. Chem. Phys. 200 (1999) 283, invited feature article.
[29] J.W. Gibbs, Am. J. Sci. Ser. 3 (16) (1878) 441.
[30] J. Dalton, A New System of Chemical Philosophy, London, 1808 (the ideas appeared first in his notebook covering 1802/04).
[31] B. Wunderlich, Thermochim. Acta 340–341 (1999) 37.
[32] H. Staudinger, Organische Kolloidchemie, third ed., Verlag, Braunschweig, 1950.
[33] H. Staudinger, J. Fritschi, Helv. Chim. Acta 5 (1922) 788.
[34] B. Wunderlich, J. Grebowicz, Adv. Polym. Sci.60–61 (1) 1984.
[35] T. Graham, Trans. Farad. Soc. (London) 151 (1861) 183.
[36] J. Timmermanns, J. Phys. Chem. Solids 18 (1961) 1.
[37] U. Gaur, B. Wunderlich, Macromolecules 13 (1980) 1618.
[38] J.A. Forrest, J. Mattsson, Phys. Rev. E 61 (2000) R53.
[39] B. Wunderlich, G. Czornyj, Macromolecules 10 (1977) 906.
[40] R. Androsch, B. Wunderlich, J. Polym. Sci., Part B: Polym. Phys., in press.
[41] J. Pak, B. Wunderlich, Macromolecules 34 (2001) 4492.
[42] J. Pak, B. Wunderlich, J. Polym. Sci., Part B: Polym. Phys. 38 (2000) 2810.
[43] H. Suzuki, J. Grebowicz, B. Wunderlich, Br. Polym. J. 17 (1985) 1.
[44] V.B.F. Mathot, J. Van Ruiten, in: V.B.F. Mathot (Ed.), Calorimetry and Thermal Analysis of Polymers, Hanser Publishers, Munich, 1993.
[45] C. Schick, A. Wurm, A. Mohammed, Coll. Polym. Sci. 279 (2001) 800.
[46] S.Z.D. Cheng, B. Wunderlich, Macromolecules 20 (1987) 1630.
[47] J. Pak, M. Pyda, B. Wunderlich, Macromolecules 36 (2003) 495.
[48] Y. Nukuchina, Y. Itoh, E.W. Fischer, J. Polym. Sci. B3 (1965) 383.
[49] E.W. Fischer, Pure Appl. Chem. 31 (1972) 113.
[50] M. Kunz, M. Möller, U.-R. Heinrich, H.-J. Cantow, Makromol. Chem. Symp. 20 (21) (1988) 147;
M. Kunz, M. Möller, U.-R. Heinrich, H.-J. Cantow, Makromol. Chem. Symp. 23 (1989) 57.
[51] B. Goderis, H. Reynaers, H. Scherrenberg, V.B.F. Mathot, M.H.J. Koch, Macromolecules 34 (2001) 1779.
[52] R. Androsch, B. Wunderlich, J. Polym. Sci., Part B: Polym. Phys., in press.
[53] J. Pak, B. Wunderlich, J. Polym. Sci., Part B: Polym. Phys. 40 (2002) 2219.
[54] R. Androsch, J. Blackwell, S.N. Chvalun, B. Wunderlich, Macromolecules 32 (1999) 3735.
[55] V.M. Litvinov, V.B.F. Mathot, Solid State Nucl. Magn. Reson. 22 (2002) 218.
[56] Y.K. Kwon, A. Boller, M. Pyda, B. Wunderlich, Polymer 41 (2000) 6237.

[57] Y. Fu, W. Chen, M. Pyda, D. Londono, B. Annis, A. Boller, A. Habenschuss, J. Cheng, B. Wunderlich, J. Macromol. Sci., Phys. B35 (1996) 37.
[58] Book of Abstracts, 17th IUPAC Conference on Chemical Thermodynamics, Concurrent with the Laehnwitz Seminar on Calorimetry: Thermodynamics and Calorimetry of Small Systems ICCT 2002, Mathematisch-Naturwissenschaftliche Fakultät, University of Rostock, Rostock, Germany, 2002, pp. 263–277.
[59] Proceedings of the International Symposium on Polymer Crystallization in Mishima, Japan, 2002; J. Macromol. Sci., Phys. Ed., in press.